ChemComm

Accepted Manuscript

ROYAL SOCIETY OF CHEMISTRY

rsc.li/chemcomm

ROYAL SOCIETY OF CHEMISTRY View Article Online
DOI: 10.1039/C8CC08446G

Journal Name

COMMUNICATION

New mechanism for the nucleation and growth of large zeolite X crystals in the presence of triethanolamine

Savannah J. Turner,[a] Jialu Chen,[a] Alexandra M. Z. Slawin[a] and Wuzong Zhou,*[a]

Received 00th January 20xx,
Accepted 00th January 20xx

DOI: 10.1039/x0xx00000x

www.rsc.org/

Large octahedral zeolite X crystals nucleate inside preformed spherical particles at the interface between an amorphous core and a shell of zeolite P nanorods. Triethanolamine enhances the sphere formation and is involved in the growth of zeolite X crystals.

Zeolites are popular industrial materials worth billions of US dollars in the global market. Although many zeolites occur naturally and can be mined, synthetic zeolites are more often used commercially due to their significantly greater purity and particle size uniformity. A fundamental understanding of zeolite growth during synthesis is becoming increasingly important to facilitate control over their properties and structures.[1] Faujasite type zeolites, such as zeolites X and Y, are amongst the most important zeolites used commercially.[2]

It has long been known that ultra-large crystals of various zeolites can be grown, when triethanolamine (TEA) is added to the reaction mixture. [3] The most prominent theory for the mechanism by which this enhanced growth occurs is that Al^{3+} cations in the gel are complexed by TEA, reducing their effective concentration.[4] This would in turn reduce the supersaturation and therefore the number of nucleation sites leading to a smaller number of crystals. This mechanism was supported by NMR results, which suggested that an Al-TEA complex may exist in the gel.

The commonly reported issue with using TEA to promote crystal growth is the formation of secondary phases. For instance, when attempting to synthesize zeolite X, zeolite P forms as a secondary phase, whose content increases with increasing the amount of TEA. [5] Another example is the synthesis of EMT type zeolite, where SOD, LTA and FAU type phases form depending on the reaction conditions in the presence of TEA.[6] When the zeolite syntheses in both of these cases are performed without the organic additive, pure phase zeolite X or zeolite EMT in relatively smaller size are produced.[5,6]

On the other hand, adding organic additives in the reaction mixtures of zeolites may enhance aggregation of the precursor molecules/ions or nanocrystallites into amorphous or polycrystalline particles. The nucleation sites of the zeolites may shift from the solution to the solid phases, leading to a reversed crystal growth route.[7] It is of interest to find whether TEA also has such an effect.

Herein, we present our recent ex-situ study of the crystal growth mechanism of zeolite X in the presence of TEA and its relation with the secondary phase zeolite P. This provides significantly greater insight into the role of TEA and reveals that the growth of the two phases are in fact heavily intertwined.

Zeolite X was hydrothermally synthesized using a modified procedure developed by Warzywoda et al.[8] The molar ratio of the chemicals in the gel used was $4.76Na_2O : 1.0Al_2O_3 : 3.5SiO_2 : 454.0H_2O : 8.0$TEA. Specimens were collected after reaction at 100°C for 1 to 14 days, and were characterised using several techniques. The details of the chemicals used, synthesis procedure and characterisation methods are given in electronic supplementary information (ESI†).

Specimen after 14 days reaction contain large particles (~60 μm in diameter) with two distinguished morphologies, octahedral and spherical, as shown in a scanning electron microscopy (SEM) image (Fig. 1a). All the peaks in the powder X-ray diffraction (XRD) pattern can be indexed to zeolite X and zeolite P (Fig. 1b). Zeolite X crystals are octahedral in shape as commonly observed and confirmed by powder XRD and SEM images of early stage samples, as well as single crystal XRD in the present work (Fig. S1, ESI†), from which the structure was determined by a structural refinement to be face-centred cubic with a = 24.846(6) Å, space group: $Fd\bar{3}m$.

To understand how these crystals developed, powder XRD patterns of the early stage samples were collected (Fig. 2). The 1 day sample is amorphous (Fig. 2a). SEM image of this sample shows some irregular aggregates of precipitate (Fig. S2a, ESI†). After 2 days reaction, very faint XRD peaks of zeolite P appear

[a] EaStChem, School of Chemistry, University of St Andrews, St Andrews, KY16 9ST, United Kingdom; E-mail: wzhou@st-andrews.ac.uk

† Electronic Supplementary Information (ESI) available: Experimental details, single crystal XRD analysis, TEM images and SAED patterns, EDX, particle size distributions, more SEM images and powder XRD patterns. See DOI: 10.1039/x0xx00000x

(Fig. 2b). The corresponding SEM images show the major phase of irregular aggregates co-existing with some spherical agglomerates (Fig. 3a). An SEM image of a cross section of a sphere (inset of Fig. 3a) shows that its surface is completely covered by short nanorods normal to the sphere surface, forming a thin crystalline crust of zeolite P, which was confirmed by a selected area electron diffraction (SAED) study later. It seems to be very likely that these zeolite P nanorods are responsible for the weak peaks in the XRD pattern of Fig. 2b.

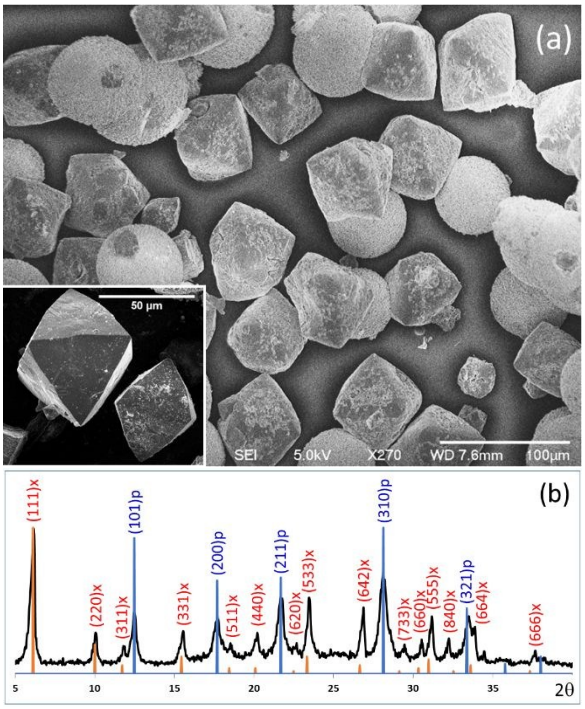

Fig. 1 (a) SEM image of the 14 days sample showing octahedral and spherical particles. The inset is an image of selected octahedral particles. (b) The powder XRD pattern of the 14 days sample indexed to zeolite X (red) and zeolite P (blue).

The intensity of the diffraction peaks of zeolite P increased significantly in the 3 days sample (Fig. 2c). This is because the number of spherical particles increases largely (Fig. S2b, ESI†) and the zeolite P nanorods grow up (Fig. 3b). The measured length of the nanorods in the 3 days sample is ca. 5 μm (Fig. 3b), while that in the 2 days sample is about 2 μm (Fig. 3a).

The spherical particles were crushed for transmission electron microscopy (TEM) examination. SAED patterns from the nanorods can be indexed to the cubic unit cell of zeolite P with a = 10.043 Å (Fig. S3, ESI†). The longitudinal axis of the nanorods is parallel to the [100] zone axis of zeolite P. Unfortunately, the crystals are very beam sensitive and no HRTEM images with lattice fringes were recorded.

Elemental distributions in the spherical particles were examined by energy dispersive X-ray (EDX) linear microanalysis (Fig. S4, ESI†) from the centre to the surface of a sphere with 110 μm in diameter and 12 μm in the thickness of zeolite P crust. The atomic ratio of Na : O : Si : Al is almost uniform from the centre to the surface. However, the intensities of the X-rays at the zeolite P crust are much higher than in the inner core. The intensities of the X-rays in the interface region between the zeolite P crust and the core are the lowest.

View Article Online DOI: 10.1039/C8CC08446G

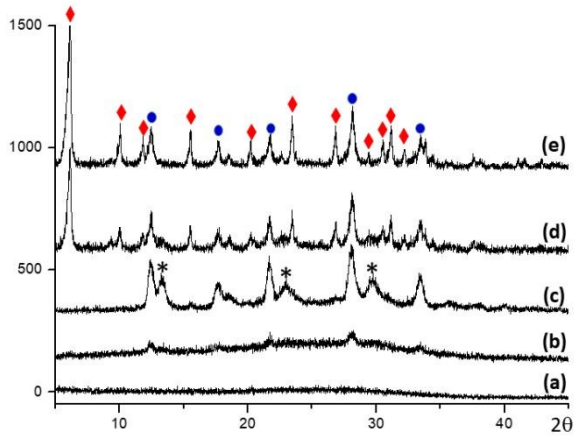

Fig. 2 Powder XRD patterns from the specimens after hydrothermal reaction for (a) 1, (b) 2, (c) 3, (d) 4 and (e) 5 days. The red diamonds indicate the peaks from zeolite X. The blue solid circles mark the peaks from zeolite P. The asterisks in (c) indicated some peaks from an unknown impurity phase.

Bearing in mind that triethanolamine molecules in the particles may be removed during drying at 100 °C, the 3 days sample was also dried at room temperature. EDX results show a significant amount of carbon. Organic/inorganic composite aggregates are confirmed (Fig. S5a, ESI†).

Two more points in the XRD patterns in Fig. 2c draw our attention. First, some extra peaks appear, implying a possible cubic phase with a = 9.481Å. The impurity should not be phillipsite (zeolite Na-PHI) which is known to form occasionally alongside zeolite P, [9] because the latter has a monoclinic unit cell with a ≈ 10.0, b ≈ 14.2, c ≈ 8.70 Å, β ≈ 125.1°. [10] On the other hand, no indication of this phase is seen in any other samples and it simply disappears from the XRD patterns (Fig. S6, ESI†) as the reaction time increased. We therefore pay no further attention to it in this study. The second point is that zeolite X does not form during the hydrothermal treatment for 3 days, but its content in 4 days sample is very high. To reveal more detailed crystal growth process of zeolite X, three more samples were prepared with reaction for 3¼, 3½ and 3¾ days.

Surprisingly, zeolite X was not detected by XRD in the 3¼ and 3½ days samples. In XRD pattern of the 3¾ days sample, a very weak peak, which can be indexed to the {111} planes of zeolite X, appears. It indicates that nucleation of zeolite X has taken place in this sample and, in the following several hours, we may see a quick growth of zeolite X (Fig. S6, ESI†).

SEM images of the 3¼ and 3½ days samples show many spherical particles without any trace of zeolite X, in agreement with the XRD results. However, in the 3 ¾ days sample, some octahedral particles appear at the surface of the spheres, like a plant growing out from soil (Fig. 3c). With further increase of growth time, in the 4 days and 5 days samples, more octahedral particles of zeolite X formed and some large particles disconnected from the spheres (Fig. 3d). The co-existence of the

View Article Online
DOI: 10.1039/C8CC08446G

zeolite P-containing spheres and octahedral zeolite X remained unchanged in all the samples with longer growth time.

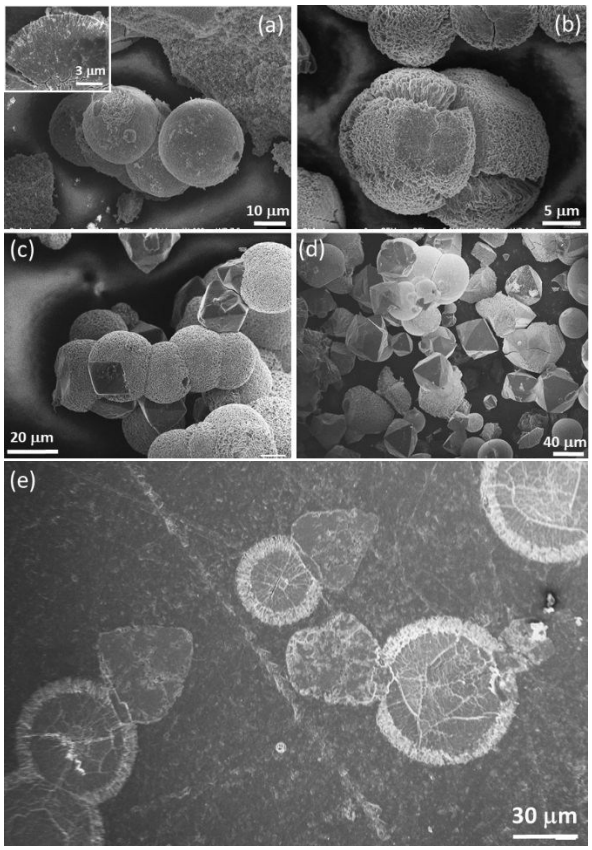

Fig. 3 Typical SEM images of early stage samples. (a) The 2 days sample. The inset is a cross section image showing surface crystallisation of a spherical particle. (b) The 3 days sample. (c) The 3 ¾ days sample. (d) The 5 days sample, and (e) a polished cross section of the 14 days sample encased in resin.

When a cross section of the particles were imaged using SEM, we can see that crystallisation of zeolite X actually starts at the interface between the core and the shell of the spherical particles (Fig. 3e). The crystal grow outwards but not inwards. Consequently, the core-shell spheres are almost intact during the crystal growth of zeolite X. The building units of zeolite X mainly came from the solution. The average size of the spheres increased from the 1 day sample to the 8 days sample, and then remained constant (Fig. S7a, ESI†).

The high stability of zeolite P as the shell of the spheres is also implied by SEM images. With increasing the reaction time, not only does the sphere size increase, but the length of the zeolite P also increases to about 20 μm in the 14 days sample (Fig. S8a,b, ESI†). A phase separation can be seen from the SEM image contrast pattern, which divided into four layers, marked A, B, C and D from the surface to the core. The zeolite P crust consists of A and B layers with relatively thinner crystals in the latter. The significant darker image contrast in the C layer is because this layer is basically amorphous with a smooth surface, containing lower concentrations of the principal metal cations. The region D shows a similar image contrast to that in region A, probably indicating that crystallisation of zeolite P may take place in the centre of spheres as well.

The crystalline crust can be easily disconnected from the amorphous core (Fig. S8c, ESI†). The zeolite P nanorods grow up into microrods via Ostwald ripening. The end of these microrods show a cross pattern formed by two edges along [010] and [001], if the view direction is defined as [100]. The exposed facets on both sides of the edges are parallel to the edges, i.e. (101), (10$\bar{1}$), (110), and (1$\bar{1}$0) (see Fig. S8d, ESI†).

Unlike the spheres, the size of the octahedral zeolite X increases with the reaction time up to 8 days, and then reduces gradually (Fig. S7b, ESI†). This reduction is due to imperfection of the particles at early stages, in which many holes can be found through the whole body (Fig. S9, ESI†). This is because TEA is involved in the particles as detected by EDX (Fig. S5b, ESI†). At later stages, TEA molecules migrate from the octahedral particles to the solution, the crystals shrank to fill these holes. When the particles were dried at 100 °C, all organic molecules would be removed, leaving some holes. No carbon was detected from these particles (Fig. S9d, ESI†). From single crystal XRD experiments, we also detected that the large octahedra are imperfect. The exposure time used had to be much longer than normal time because the intensities of the diffraction spots are very weak (Fig. S10, ESI†).

EDX results from zeolite P on the sphere surface and zeolite X, more than 10 particles being selected for each phase, indicate that the Si : Al ratios are quite similar, 1.54±0.08 and 1.6±0.2, respectively (Fig. S9c,d, ESI†). Therefore, it is unlikely that the Si : Al ratio makes an important influence to the early appearance of zeolite P.

The experimental data we observed in this work enable us to propose a multi-step crystal growth mechanism of zeolite X in the presence of TEA (Fig. 4).

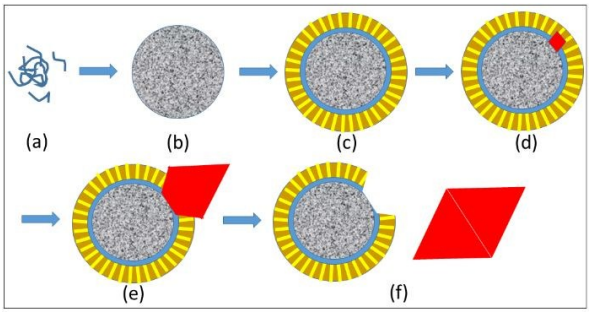

Fig. 4 Schematic drawing of the proposed formation mechanism of octahedral zeolite X crystals. (a) Loose precipitate of precursors and TEA. (b) Amorphous spherical aggregate. (c) Surface crystallisation, forming a zeolite P nanorod crust. (d) Nucleation of zeolite X at the interface of the zeolite P crust and the amorphous core. (e) Growth of zeolite X. (f) Separation of the sphere and the zeolite X crystal.

Step 1. The precursor molecules/ions including TEA molecules aggregate together into loose precipitate due to strong inter-molecular interactions (Fig. 4a). Forming Al-TEA complex in the solution and in the precipitate is quite possible.

Step 2. The TEA enhanced aggregates increase their density to form non-crystalline spheres (Fig. 4b). Naturally, the

concentration of the precursors in the solution is greatly reduced. Nucleation in the solution is suppressed. In fact, at these early stages, individual crystals of either zeolite P or zeolite X were not observed.

Step 3. Nucleation followed by crystallisation takes place on the sphere surface, forming a crust of radially arranged zeolite P nanorods (Fig. 4c). It is more difficult to take place inside the spheres, since there is restricted space, limited mass transportation, less help from the solvent. The prioritized appearance of zeolite P is probably governed by the high density of the precursors in the spheres, as reported previously that high concentration of [Si, Al] and high temperature help the formation of zeolite P. [11] The possible reason is that zeolite P has a much higher density, 15.3 (Si,Al)/1000Å^3, than that of zeolite X, 12.7 (Si,Al)/1000Å^3. Surface crystallisation of disordered spherical aggregates is an important step in reversed crystal growth, forming a thin single crystal polyhedral shell.[12] In the present work, the surface crystallisation does not lead to a single crystal shell. The extension of the crystallisation on the sphere surface is suppressed by the adsorbed TEA molecules.

Step 4. Nucleation of zeolite X occurs at the interface between zeolite P crust and the amorphous core in the spheres (Fig. 4d), where the relatively lower density and lower concentrations of the precursors are suitable for development of zeolite X. Only one zeolite X crystal normally forms in each sphere. Consequently, the total number of zeolite X crystals is greatly reduced, resulting in large crystals.

Step 5. Zeolite X octahedral particles grow outwards fast (Fig. 4e) and do not grow inwards due to a high density of the sphere centre. The extension of crystallisation to the centre may build up a pressure. A similar phenomenon was found previously in reversed crystal growth of zeolite A.[13] Deposition of Al^{3+} in the form of Al-TEA complex and very fast growth rate result in capture of a large amount of TEA molecules inside the zeolite X particles.

Step 6. Zeolite X crystals drop down from the zeolite P-containing spheres. Perfect octahedral morphology can be achieved in the solution. The crystals shrink to reduce the porosity, finally forming real single crystals (Fig. 4f).

In conclusion, some novel phenomena observed in the crystal growth of zeolites X and P the presence of TEA allow us to propose a new formation mechanism of these zeolites. We have confirmed several points. First, TEA functions as an agglomeration matrix during the crystal growth, enhancing the formation of spherical aggregates, including all the precursors. The concentrations of the precursors in the solution are largely reduced. Therefore, nucleation of zeolites does not occur in the solution. Second, surface crystallisation of zeolite P nanorods generates a region at the interface between the crystalline shell and the amorphous core, which is suitable for nucleation of zeolite X. Third, all zeolite X crystals grow on the surface of the spheres. No phase transformation from zeolite P to zeolite X was not observed. This work may shed light on growth of other zeolites in presence of TEA.

Conflicts of interest

There are no conflicts to declare.

View Article Online
DOI: 10.1039/C8CC08446G

Notes and references

1 J. Grand, H. Awala and S. Mintova, *CrystEngComm*, 2016, **18**, 650–664.
2 E. Flanigen, R. Broach and S. Wilson, in *Zeolites in Industrial Separation and Catalysis*, ed. S. Kulprathipanja, Wiley-VCH Verlag GmbH & Co. KGaA, Weinheim, Germany, 2010, pp. 1–26.
3 W. Schmitz, J. Kornatowski and G. Finger, *Cryst. Res. Technol.*, 1987, **22**, 35–41; G. Scott, A. Dixon, A. Sacco and R. Thompson, *Stud. Surf. Sci. Catal*., 1989, **49**, 363–372; D. Fu, J. Schmidt, Z. Ristanović, A. Chowdhury, F. Meirer and B. Weckhuysen, *Angew. Chem. Int. Ed*., 2017, **56**, 11217–11221; E. Basaldella and J. Tara, *Mater. Lett*., 1998, **34**, 119–123.
4 G. Scott, R. W. Thompson, A. Dixon and A. Sacco, *Zeolites*, 1990, **10**, 44–50.
5 R. Tekin, N. Bac, J. Warzywoda and A. Sacco, *J. Cryst. Growth*, 2015, **411**, 45–48.
6 V. Georgieva, A. Vicente, C. Fernandez, R. Retoux, A. Palčić, V. Valtchev and S. Mintova, *Cryst. Growth Des*., 2015, **15**, 1898–1906.
7 X. Y. Chen, M. H. Qiao, S. H. Xie, K. N. Fan, W. Z. Zhou and H. Y. He, *J. Am. Chem. Soc*., 2007, **129**, 13305–13312; J. F. Yao, D. Li, X. Y. Zhang, C. H. Kong, W. B. Yue, W. Z. Zhou and H. T. Wang, *Angew. Chem. Int. Ed*., 2008, **47**, 8397–8399.
8 J. Warzywoda, N. Baç and A. Sacco, *J. Cryst. Growth*, 1999, **204**, 539–541.
9 N. Musyoka, L. Petrik, W. Gitari, G. Balfour and E. Hums, *J. Environ. Sci. Heal*. Part A, 2012, **47**, 337–350.
10 E. Passaglia, A. F. Gualtieri and E. Galli, in *Natural Zeolites for the Third Millennium.* Edi. C. Colella and F. A. Mumpton, De Frede Editore, Napoli, Italy. 2000, pp 259-267.
11 Y.-G. Chen, W. Kang, H.-J. Han, Y.-N. Zhang, H.-Y. Wang, T.-T. Xu, X.-Q. Yang and H. Song, *J. Fuel Chem. Techno*., 2017, **45**, 1251–1259.
12 W. Z. Zhou, *Adv. Mater*. 2010, **22**, 3086–3092.
13 H. Greer, P. S. Wheatley, S. E. Ashbrook, R. E. Morris and W. Z. Zhou, *J. Am. Chem. Soc*., 2009, **131**, 17986–17992.

View Article Online
DOI: 10.1039/C8CC08446G

The Table of Contents (TOC)

New mechanism for the nucleation and growth of large zeolite X crystals in the presence of triethanolamine

Savannah J. Turner, Jialu Chen, Alexandra M. Z. Slawina and Wuzong Zhou

Zeolite X crystals nucleate inside preformed spherical particles in between the amorphous core and the shell of zeolite P nanorods.